Validated Modelling of Electrochemical Energy Storage Devices

by

Niklas Mellgren

September 2009
Technical Reports from
Royal Institute of Technology
Department of Mechanics
SE-100 44 Stockholm, Sweden

Typsatt i LaTeX.

Akademisk avhandling som med tillstånd av Kungliga Tekniska Högskolan i Stockholm framlägges till offentlig granskning för avläggande av teknologie licentiatsexamen fredagen den 25 september 2009 kl 10.15 i sal D3, Lindstedtsvägen 5, Kungliga Tekniska Högskolan, Stockholm.

Universitetsservice US-AB, Stockholm 2009

Validated Modelling of Electrochemical Energy Storage Devices

Niklas Mellgren
Department of Mechanics
Royal Institute of Technology
SE-100 44 Stockholm, Sweden

Abstract

This thesis aims at formulating and validating models for electrochemical energy storage devices. More specifically, the devices under consideration are lithium ion batteries and polymer electrolyte fuel cells.

A model is formulated to describe an experimental cell setup consisting of a $Li_xNi_{0.8}Co_{0.15}Al_{0.05}O_2$ composite porous electrode with three porous separators and a reference electrode between a current collector and a pure Li planar electrode. The purpose of the study being the identification of possible degradation mechanisms in the cell, the model contains contact resistances between the electronic conductor and the intercalation particles of the porous electrode and between the current collector and the porous electrode. On the basis of this model formulation, an analytical solution is derived for the impedances between each pair of electrodes in the cell. The impedance formulation is used to analyse experimental data obtained for fresh and aged $Li_xNi_{0.8}Co_{0.15}Al_{0.05}O_2$ composite porous electrodes. Ageing scenarios are formulated based on experimental observations and related published electrochemical and material characterisation studies. A hybrid genetic optimisation technique is used to simultaneously fit the model to the impedance spectra of the fresh, and subsequently also to the aged, electrode at three states of charge. The parameter fitting results in good representations of the experimental impedance spectra by the fitted ones, with the fitted parameter values comparing well to literature values and supporting the assumed ageing scenario.

Furthermore, a steady state model for a polymer electrolyte fuel cell is studied under idealised conditions. The cell is assumed to be fed with reactant gases at sufficiently high stoichiometric rates to ensure uniform conditions everywhere in the flow fields such that only the physical phenomena in the porous backings, the porous electrodes and the polymer electrolyte membrane need to be considered. Emphasis is put on how spatially resolved porous electrodes and nonequilibrium water transport across the interface between the gas phase and the ionic conductor affect the model results for the performance of the cell. The future use of the model in higher dimensions and necessary steps towards its validation are briefly discussed.

Descriptors

lithium ion battery, polymer electrolyte fuel cell, modelling, model validation, parameter fitting.

Preface

This licentiate thesis seeks to formulate and validate models for two types of electrochemical energy storage devices, namely, lithium ion batteries and polymer electrolyte fuel cells. The thesis is divided into two parts. The first part provides an introduction to electrochemical energy storage devices and tools for their study, a summary of the results obtained in the three scientific papers which are appended in the second part and a brief discussion of future work.

September 2009, Stockholm
Niklas Mellgren

Appended papers

Paper 1. Niklas Mellgren, Shelley Brown, Michael Vynnycky and Göran Lindbergh, *Impedance as a Tool for Investigating Aging in Lithium-Ion Porous Electrodes: I. Physically Based Electrochemical Model*, J. Electrochem. Soc., **155** (4) A304-A319 (2008).

Paper 2. Shelley Brown, Niklas Mellgren, Michael Vynnycky and Göran Lindbergh, *Impedance as a Tool for Investigating Aging in Lithium-Ion Porous Electrodes: II. Positive Electrode Examination*, J. Electrochem. Soc., **155** (4) A320-A338 (2008).

Paper 3. Niklas Mellgren, Michael Vynnycky and Anders Dahlkild, *Porous Electrode and Nonequilibrium Water Transport Modelling in Polymer Electrolyte Fuel Cells*, manuscript.

Division of work between authors

Most of the work presented in this thesis is a result of a collaboration between the author of this thesis, Niklas Mellgren (NM), and Dr. Shelley Brown (SB). Docent Michael Vynnycky (MV) and Docent Anders Dahlkild (AD) have acted as supervisors of NM while Prof. Göran Lindbergh (GL) supervised the work by SB.

Paper 1. The model was formulated by NM and SB. The analytical solution was derived by NM. The parameter values were estimated by SB. The model was implemented by NM and SB. The parametric study was performed by NM with feedback from SB. The paper was written by NM with input from SB and feedback from SB, MV and GL.

Paper 2. The experiments were performed by SB. The optimisation strategy was implemented by NM. The parameter fitting was undertaken by SB with feedback from NM. The paper was written by SB with feedback from NM, MV and GL.

Paper 3. The model was formulated by NM. The parameter values were estimated by NM. The model was implemented by NM. The parametric study was performed by NM. The paper was written by NM with input from MV and feedback from MV and AD.

Contents

Part I

Introduction and Summary

CHAPTER 1

Electrochemical Energy Storage

Access to renewable energy sources like solar, wind, tidal and wave energy sources is generally restricted both temporally and spatially. They fluctuate more or less predictably in time and are restricted to certain sites. Solutions to redistribute energy from such sources could involve electrochemical energy storage devices which may thus be a key component on the way to a sustainable society. Also, in the light of global warming, industry is under pressure to reduce or eliminate emissions in residential power generation and transportation. Finally, the steadily increasing usage of personal electronic devices increases demands on portable electric energy sources. These are all cases in which electrochemical energy storage devices can play to their strengths.

Electrochemical energy storage devices are classically divided into batteries, fuel cells and supercapacitors, although there are also hybrid devices. Batteries and fuel cells both convert chemical energy into electric energy and heat in an electrochemical reaction. They mainly differ in where the reactants and products for that reaction are stored. For a battery they are stored inside the cell while for a fuel cell they are being continuously fed into and removed from the cell. On the other hand, supercapacitors store energy in their electrochemical double layers and require no reactions to operate even though fast adsorption processes may effectively contribute to the capacitance of the cell.

1.1 Lithium ion batteries

In a lithium ion battery (LIB) both the reactants and the products take the form of lithium which is intercalated in two different host materials, that is intercalation materials. Intercalated lithium is mobile and may be transported by diffusion inside an intercalation particle. If such a particle is brought into contact with a suitable ionic conductor, that is electrolyte, the intercalated lithium may undergo a reversible charge transfer reaction at the particle surface and enter the electrolyte as a lithium ion, leaving an electron behind. During the discharge of a LIB lithium moves from the intercalation particles of the negative electrode to those of the positive electrode. In the process lithium

ions are transported through the electrolyte and electrons move through an external circuit from where they are left behind by the lithium ions in the negative electrode to where they recombine with the lithium ions in the positive electrode. The reactions, in units of moles, can be written as follows

$$\begin{aligned} Li_x I_n &\rightleftharpoons Li_{x-z} I_n + z\, Li^+ + z\, e^- \,, && \text{(negative electrode)} \\ Li_y I_p + z\, Li^+ + z\, e^- &\rightleftharpoons Li_{y+z} I_p \,, && \text{(positive electrode)} \\ Li_x I_n + Li_y I_p &\rightleftharpoons Li_{x-z} I_n + Li_{y+z} I_p \,, && \text{(total)} \end{aligned}$$

where x and y are fractions representing the amount of lithium in the negative and the positive intercalation materials, I_n and I_p, respectively, and z is a fraction representing the amount of transferred lithium.

The setup of a LIB consists of five domains, namely, two porous electrodes which are held apart by a porous separator and placed between two current collectors. In addition, the pore space of the three porous media is filled with a liquid electrolyte. Note that while it is also possible to use gel or polymer electrolytes, in this work the term LIB denotes battery technology based on liquid electrolytes only. Alternatively, the setup can be characterised as a structure of phases that penetrate each other across domain boundaries. In the porous electrodes the electronic and the ionic conductors provide pathways for electrons and lithium ions, respectively, to and from the intercalation material. It should be noted that the electronic conductor and the intercalation material do not necessarily need to be distinct phases provided that the electronic conductivity of the intercalation material is sufficiently high. Furthermore, the electrical insulator of the porous separator prevents the cell from short-circuiting. An attempt at merging these two points of view is shown in Fig. 1.1(a). The principle of operation of a LIB is illustrated in Fig. 1.1(b) where Li_{in} and Li_{ip} are intercalated lithium in the negative and the positive electrode, respectively. The figure describes the situation for the discharge of a LIB; during the charging all processes are reversed, the anode and the cathode switch their roles and the battery consumes electric energy.

1.2 Polymer electrolyte fuel cells

The anode and the cathode of a polymer electrolyte fuel cell (PEFC) are fed with gaseous hydrogen and oxygen, respectively, which are transported to the catalyst sites of the respective electrode where they react according to

$$\begin{aligned} 2\, H_2 &\rightleftharpoons 4\, H^+ + 4\, e^- \,, && \text{(anode)} \\ O_2 + 4\, H^+ + 4\, e^- &\rightleftharpoons 2\, H_2O \,, && \text{(cathode)} \\ 2\, H_2 + O_2 &\rightleftharpoons 2\, H_2O \,. && \text{(total)} \end{aligned}$$

The hydrogen ions, that is protons, produced in the anode reaction are transported to the cathode through the polymer electrolyte membrane which acts as

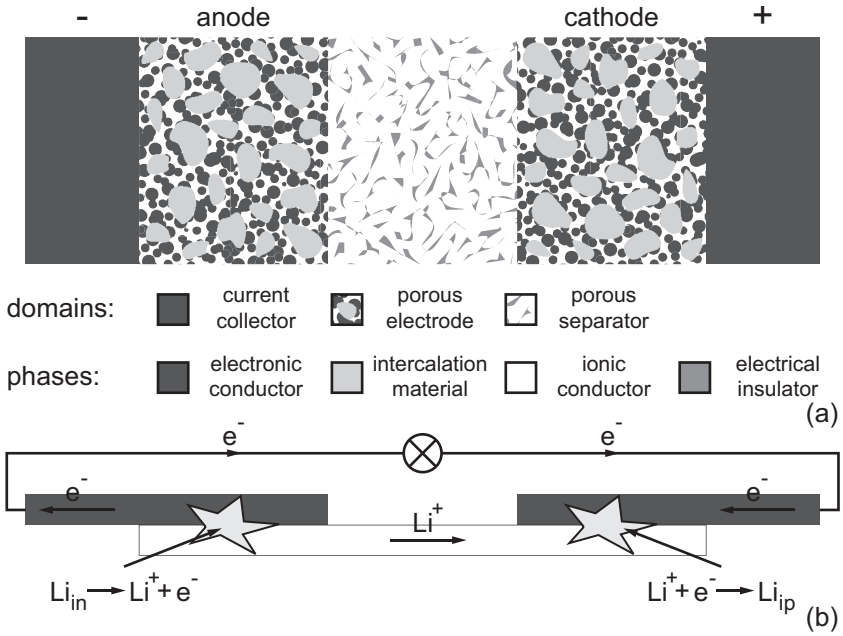

Figure 1.1: LIB setup (a) and principle of operation (b) during discharge.

an ionic conductor while the electrons move through an external circuit. The water produced in the cathode reaction may take on a gaseous or a liquid form depending on the conditions in the cell and needs to be removed by the gases leaving the cell. Liquid water may partially or completely block the transport of oxygen to the cathode, a phenomenon called flooding, leading to losses in or even failure of the operation. On the other hand, the polymer electrolyte membrane needs to be hydrated in order for it to retain its ionic conductivity and thus the inlet gases are typically humidified. Consequently, the management of water is crucial for the successful operation of a PEFC. Although a PEFC could in principle be operated in the reverse direction to electrolyse water, the design specifications for such an operation are quite different from those for normal operation and therefore a typical PEFC would not be able to do so efficiently.

The setup of a PEFC is made up of seven domains, namely, two porous electrodes separated by a polymer electrolyte membrane and placed between two porous backings which are in contact with two current collectors with flow fields. The flow fields can take the form of channel networks grooved into the current collectors or may be provided by electronically conductive porous nets. The pore systems of the porous backings and the porous electrodes

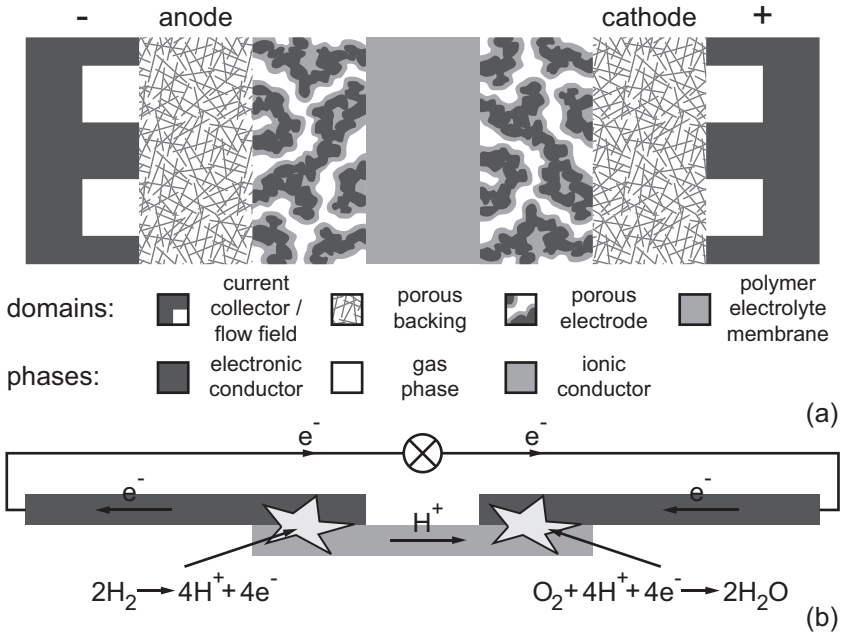

Figure 1.2: PEFC setup (a) and principle of operation (b).

provide routes of transport for the reactant gases from the flow fields to the catalyst particles in the porous electrodes. Here, the electronic and the ionic conductors serve as pathways for the electrons and the protons, respectively. A combined illustration of the domains and the phases is provided by Fig. 1.2(a). In addition, Fig. 1.2(b) shows the principle of operation of a PEFC.

1.3 Validated modelling

Models can be used to improve the understanding of the operation of electrochemical energy storage devices, including both individual physical phenomena and their interplay. Furthermore, they can be a valuable tool to design the setup and the operational conditions of such a device. Before models can be reliably used in this way, they need to be validated against experimental data. Validation will generally be necessary to confirm model concepts, equations and parameter values.

The work presented in this thesis seeks to provide validated models for LIBs and PEFCs. In particular, validated modelling is used to investigate the effects of ageing in a LIB. In addition, a model is formulated and investigated for a

PEFC and steps towards its validation are discussed.

CHAPTER 2

Models

The physical phenomena governing the performance of batteries and fuel cells are quite similar and can be described using common basic models. Other model features depend on the intended application and the aim of the investigation.

2.1 Multicomponent mass transport

Multicomponent mass transport occurs, for example, both in the liquid electrolyte in the pores of a LIB and in the gas phase in the pores and channels of a PEFC. The common starting point for the treatment of multicomponent mass transport in these cases are the generalised Maxwell-Stefan (GMS) equations [1]. These equations are essentially balances between the driving forces which induce a motion of the individual components with respect to each other and the friction forces which resist this motion and arise from the exchange of momentum between the components. In the liquid electrolyte of a LIB, including non-ideal composition gradients and an electric potential gradient as driving forces and approximating the electrolyte as electrically neutral then leads to the concentrated electrolyte equations [2]; and in the gas phase of a PEFC, including ideal composition gradients and a pressure gradient as driving forces results in the Maxwell-Stefan equations for ideal gas mixtures.

However, an additional complication arises from the interaction of the gas components with the walls in the porous structures of a PEFC. As the size of the pores becomes small in comparison with the mean free path lengths in the gas, the collisions of the gas molecules with the walls become far more frequent than the collisions of the gas molecules with each other. In this regime, the transport of the gas components is governed by Knudsen diffusion. But also for significantly larger pores the interaction of the gas components with the walls adds an additional effect since the gas mixture does not satisfy the conventional no-slip condition at the walls. This slippage which manifests itself in Graham's relation is usually negligible if the flow is dominated by convection, such as in the gas channels of a PEFC, but may be significant if the flow is

dominated by diffusion, such as in the porous structures of a PEFC. A model which encompasses Maxwell-Stefan and Knudsen diffusion and obeys Graham's relation can be formally derived from the GMS equations, yielding the dusty gas model equations[3].

The GMS equations and their derivatives only describe the relative motion of the involved components and thus they must be complemented by an additional relation. This additional relation can take the form of a flux restraint, such as setting the flux of solvent equal to zero in the case of a LIB, or a momentum equation, such as the Navier-Stokes equation for the flow of gas in the gas channels of a PEFC or Darcy's equation for the flow of gas in the porous structures of a PEFC.

2.2 Porous electrodes

A typical planar electrode can be characterised as the interface between an electronic and an ionic conductor at which an electrochemical reaction may take place. As such it must be accessible by the reactants and allow removal of the products, that is electrons in the electronic conductor, ions in the ionic conductor and possibly uncharged species in either phase or additional phases. Additional phases which provide reactants, take care of products or simply act as catalysts in the reaction may make a purely planar electrode impractical or impossible. Also, it may be desirable to increase the area of the reaction surface in order to decrease the local current densities and thus the surface overpotentials, that is losses. This motivates the use of porous electrodes which are quite common in technical applications.

In porous electrodes, the electronic and the ionic conductors should form continuous matrices that percolate the entire porous electrode volume and interpenetrate each other effectively. In this way porous electrodes provide a high specific surface area of the reaction surface which is easily accessible from either phase. Further structural features depend on the type of the porous electrode. In a LIB, the charge transfer reaction occurs at the interface between the ionic conductor and intercalation particles which are in contact with the electronic conductor while in a PEFC, it occurs at the interface between the ionic conductor and catalyst particles which are attached to the electronic conductor. The porous electrodes of a PEFC additionally have to provide a continuous pore system for the transport of gaseous reactants and products to and from the reaction surface, respectively.

2.3 Lithium ion batteries

The model presented and examined in Papers 1 and 2, respectively, describes an experimental cell setup consisting of a $\mathrm{Li}_x\mathrm{Ni}_{0.8}\mathrm{Co}_{0.15}\mathrm{Al}_{0.05}\mathrm{O}_2$ composite

porous electrode with three porous separators and a reference electrode between a current collector and a pure Li planar electrode. On the macroscopic scale, the porous electrode and the porous separators are modelled by means of porous electrode theory [2], using Ohm's law in the electronic conductor and concentrated electrolyte theory in the ionic conductor. On the microscopic scale, the model is more diverse. The charge transfer reactions on the lognormally or Dirac distributed spherical or flake-shaped intercalation particles in the porous electrode and on the planar electrode are modelled with Butler-Volmer kinetic expressions. The model describing the double layer current on the intercalation particles, the planar electrode, the electronic conductor and the current collector allows for a mixed contribution by anions and cations. The transport of intercalated lithium in the intercalation particles is modelled using Fick's law. Since the purpose of the study was to identify possible degradation mechanisms in the cell, the model contains contact resistances between the electronic conductor and the intercalation particles, between the current collector and the electronic conductor and between the current collector and the ionic conductor.

2.4 Polymer electrolyte fuel cells

Paper 3 studies the idealised operation of a PEFC in which the cell is being fed with reactant gases at such high stoichiometric rates that the gas compositions at the boundaries of the porous backings facing the flow fields are the same as at the gas inlets. In such a mode of operation the performance of the cell should be independent of the type and the geometry of the flow fields. In addition, the model equations only need to be solved in the cell normal direction. Moving from the outside to the inside of the cell, it is comprised of two porous backings, two porous electrodes and a polymer electrolyte membrane. The model is first formulated for the porous electrodes and the model equations for the remaining domains then follow as special cases thereof. The transport of gas components in the porous backings and the porous electrodes is described by the dusty gas model. The pores of the porous backings are assumed to be so large that Knudsen diffusion can be neglected and the appropriate limit of the dusty gas model is used. In the ionic conductor, the transport of water is governed by diffusion and the water drag effect [4]. The transport of charge in the electronic and the ionic conductor is modelled using Ohm's law, where the ionic conductivity of the ionic conductor depends on its water content [4]. The water uptake isotherm of the ionic conductor is given by an extended Flory-Huggins model [5]. Both electrode reactions are formally treated as elementary steps to arrive at Butler-Volmer kinetic expressions which are subsequently approximated by linear and Tafel kinetics. Finally, the water flux across the interface between the gas phase and the ionic conductor is inhibited by a mass transfer resistance resulting in a nonequilibrium of the water between the gas phase and the ionic conductor [6].

CHAPTER 3

Methods

This chapter briefly discusses a few methods that are useful in formulating or analysing models of a range of electrochemical systems. In particular, the method of volume averaging is implicit in the model formulations in Papers 1 and 3. The analysis considered in Papers 1 and 2 is based on electrochemical impedance spectroscopy. Additionally, parameter fitting is an essential technique employed in Paper 2.

3.1 Volume averaging

The geometrical details of the porous structures encountered in a LIB or a PEFC are typically small, complex and random. While it is possible to resolve the geometry of all phases, formulate the governing equations for all phases and phase boundaries and solve the resulting generally coupled system of equations, the computational cost is enormous. In addition, the detailed information provided by such a procedure is usually not even necessary and suitably averaged quantities are sufficient.

In volume averaging theory [7], all unknown quantities are spatially integrated over the phase in which they are defined within a representative volume around a variable point in space. The intrinsic volume average of a particular quantity is then defined by dividing the corresponding integral by the volume of the associated phase within the representative volume. In order to obtain the superficial volume average, the integral is instead divided by the total representative volume. As a result, these averages are simply related by the volume fraction of the phase in question. The volume averaging operator is applied to all governing equations and the resulting equations are rewritten in terms of the average quantities. In general, this procedure results in terms which cannot be written exclusively in terms of the average quantities but also include the deviations from these averages and which have to be modelled in some way. This kind of closure problem is also encountered in other areas of engineering, such as turbulence modelling in fluid mechanics.

Some aspects of the formulation of the governing equations for a porous structure, such as the boundary and transitional conditions, can be simplified by using intrinsic and superficial averages for all scalar-type and vector-type quantities, respectively. For this choice of quantities, the main effect of averaging transport equations such as diffusion and conduction equations is the replacement of transport properties such as diffusivities and conductivities by corresponding effective properties. A widely used relation between the effective and the bulk values of such transport properties, particularly in the absence of a more detailed study of the porous medium at hand, is given by the Bruggeman relation [8,9].

3.2 Electrochemical impedance spectroscopy

Electrochemical impedance spectroscopy (EIS) [10] is a powerful analytical method for the investigation of electrochemical cells. The cell under consideration is usually in an equilibrium state or operated in a steady state. In applying this method, a sinusoidal perturbation of small amplitude is introduced in the cell potential or the cell current density and the quasi-steady response in the respective other quantity is measured. If the amplitude and the phase angle of the perturbations are combined by means of complex notation, the cell impedance can be defined as the ratio between the perturbations of the cell potential and the cell current density.

By measuring the impedance for a series of frequencies spanning several orders of magnitude, that is the impedance spectrum, it is possible to distinguish between processes which are associated with different time scales. In fact, the ability to isolate the effects of individual processes and parameters is probably one of the most useful features of this method. The results of EIS measurements can only be meaningfully interpreted with the aid of mathematical models. However, different physical phenomena may have similar impacts or overlapping intervals of influence on the impedance spectrum, particularly in complex electrochemical cells. In order to successfully analyse such systems, it is therefore important to combine EIS with other electrochemical and material characterisation methods to independently study effects and determine or estimate parameters of individual processes. Also, using reference electrodes may help to isolate the effects of individual components. In combination with other suitable methods, EIS can be an excellent tool to quantitatively examine electrochemical cells.

3.3 Parameter fitting

Several factors have an impact on the degree of success of a parameter fitting process. First of all, the experimental data, the model formulation and the

fitting parameters have to be well matched. The model formulation must be able to reproduce effects seen in the experimental data. Or, conversely, the experimental data must provide information on the effects described in the model formulation. Choosing a suitable set of fitting parameters is intimately connected to this issue. A suitable set should result in an acceptable level of discrepancy between the experimental and the modelling results for realistic values and tolerable uncertainties of the fitting parameters. Consequently, designing the experiments, formulating the model and choosing the fitting parameters is an iterative process.

Optimal parameter values are found by minimising a suitable objective function. Objective functions typically follow from maximum likelihood estimators based on the standard deviations of the experimental data points. In those cases where these standard deviations are not known, they need to be estimated. For example, estimating them as constant or proportional to the experimental values leads to least squares formulations based on absolute or relative errors, respectively. Since the estimation method may have a significant impact on the optimal parameter values, it needs to be considered carefully.

In minimising the objective function of a parameter fitting problem, it is quite common to encounter numerous local minima, particularly as the number of fitting parameters increases. Furthermore, for some parameters it may even be difficult to estimate an order of magnitude. As a result, the optimal parameter values returned by a deterministic optimisation method may strongly depend on the initial guess. This problem may be overcome by creating a set of random initial guesses and choosing the most optimal parameter values of all optimisation processes. As the influence of the initial guess on the optimal parameter values increases, however, a stochastic optimisation method, such as a simulated annealing or genetic algorithm method[11], becomes more advantageous. In order to increase the performance of such a rather slow optimisation method, it can be hybridised by using a deterministic optimisation method to optimise in local minima and leaving the search for the global minimum to the stochastic optimisation method.

Once the optimal parameter values have been found, it remains to estimate their confidence intervals and to attempt to objectively judge how good a fit has been achieved, that is whether the model formulation was a good choice[12]. For model formulations in which the measured quantities depend strongly nonlinearly on the fitting parameters, these questions are not straightforward to answer. In practice, one may have to resort to subjectively comparing the experimental and the modelling results and confirming that the optimal parameter values compare well enough with typical literature values, provided that such values exist.

CHAPTER 4

Results and Discussion

A summary of the most important results of the appended papers and some related discussion is given in this chapter.

4.1 Lithium ion batteries

Paper 1 presents a model describing a $Li_xNi_{0.8}Co_{0.15}Al_{0.05}O_2$ composite porous electrode with three porous separators and a reference electrode between a current collector and a pure Li planar electrode. The model formulation is used to derive an analytical solution for the impedances between each pair of electrodes in the cell. The effect of selected components of the physical model on the impedance spectrum of the porous electrode is studied using parameter values obtained from Paper 2. In particular, it is shown that the main ageing-related parameters have quite distinct effects on the impedance spectrum, which is essential for the regression of experimental data and the study of ageing hypotheses undertaken in Paper 2.

In Paper 2, the cell setup modelled in Paper 1 is used to experimentally study fresh and aged $Li_xNi_{0.8}Co_{0.15}Al_{0.05}O_2$ composite porous electrodes. Impedance spectra are presented for a fresh electrode and an electrode which has been aged in an accelerated hybrid electric vehicle lifetime matrix. For a detailed description of the ageing and experimental procedures see Paper 2. A hybrid genetic optimisation technique is used to simultaneously fit the model to the impedance spectra of the fresh electrode at three states of charge. Figs. 4.1-4.3 present the spectra of the experimental and the fitted impedances of the positive porous electrode, $\mathcal{Z}_p$, for the fresh electrode at three states of charge. Here, the spectra are plotted in the form of Nyquist plots, that is parametric plots of the negative imaginary against the real part of the impedance in which the parameter being varied is the frequency of the perturbation, f. As can be seen, the regression results in a good representation of the experimental impedance spectra by the fitted ones. In addition, the fitted parameter values compare well to literature values.

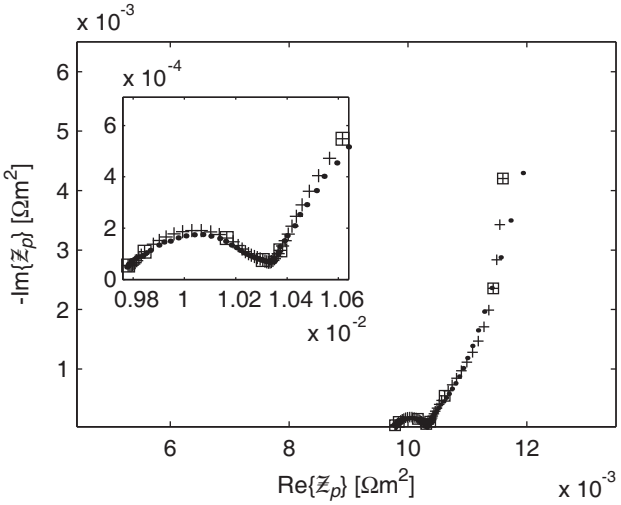

Figure 4.1: Spectra of the experimental (•) and the fitted (+) impedances of a fresh $Li_xNi_{0.8}Co_{0.15}Al_{0.05}O_2$ positive porous electrode at a state of charge corresponding to $x = 0.54$; $f = 1000$, 125, 10, 1, 0.1, 0.01, 0.001 and 0.0005 Hz marked with □.

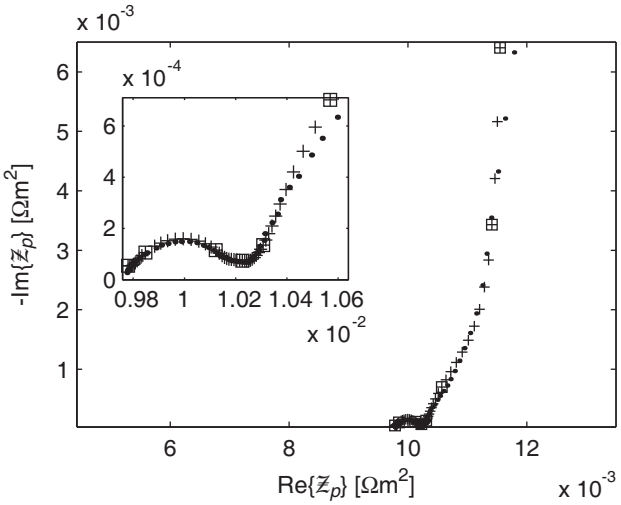

Figure 4.2: Spectra of the experimental (•) and the fitted (+) impedances of a fresh $Li_xNi_{0.8}Co_{0.15}Al_{0.05}O_2$ positive porous electrode at a state of charge corresponding to $x = 0.43$; $f = 1000$, 125, 10, 1, 0.1, 0.01, 0.001 and 0.0005 Hz marked with □.

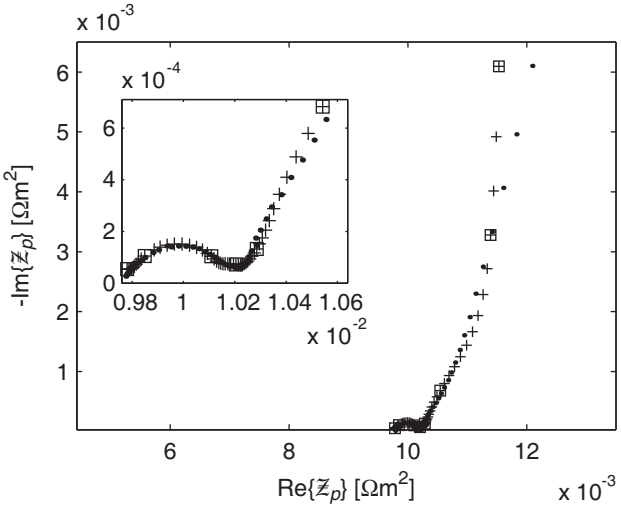

Figure 4.3: Spectra of the experimental (•) and the fitted (+) impedances of a fresh $Li_xNi_{0.8}Co_{0.15}Al_{0.05}O_2$ positive porous electrode at a state of charge corresponding to $x = 0.33$; $f = 1000$, 125, 10, 1, 0.1, 0.01, 0.001 and 0.0005 Hz marked with □.

Ageing scenarios are formulated based on experimental observations and related published electrochemical and material characterisation studies. The main effects of ageing are thought to be related to changes in the contact resistances between the intercalation particles and the electronic conductor, which may depend on the state of charge of the electrode, between the current collector and the electronic conductor and between the current collector and the ionic conductor. Furthermore, intercalation particles may lose contact to the porous electrode and thus become unavailable to the process, effectively leading to changes in their distribution. The model is simultaneously fitted to the impedance spectra of the aged electrode at three stages of charge according to a number of different ageing scenarios. The results of assuming the main ageing scenario are shown in Fig. 4.4 in which the spectra of the experimental and the fitted impedances of the positive porous electrode are plotted in the form of Nyquist plots for the aged electrode at three stages of charge. The resulting fitted impedance spectra agree well with the experimental ones and the fitted parameter values are consistent with the assumed ageing scenario. While the developed ageing scenario is shown to be plausible, the results cannot rule out other ageing scenarios. In particular, many quite different effects of ageing may have similar impacts on the impedance spectrum or may even be modelled in identical ways. Nevertheless, in combination with additional electrochemical

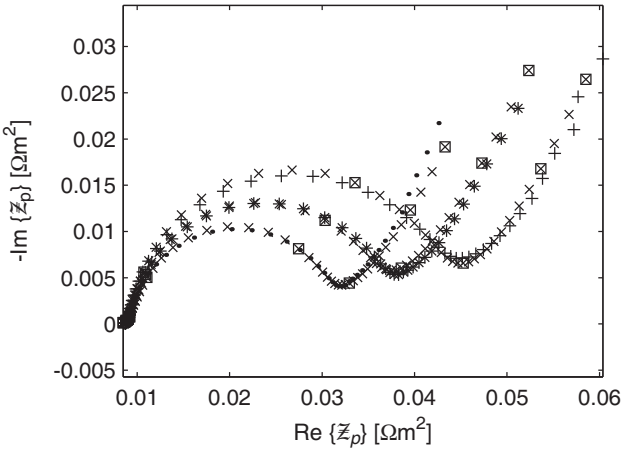

Figure 4.4: Spectra of the experimental (•, ∗, +) and the fitted (×) impedances of an aged $Li_xNi_{0.8}Co_{0.15}Al_{0.05}O_2$ positive porous electrode at states of charge corresponding to $x = 0.54$ (•), $x = 0.43$ (∗) and $x = 0.33$ (+); $f = 1000$, 125, 10, 1, 0.1, 0.01, 0.001 and 0.0005 Hz marked with □.

and material characterisation methods the suggested methodology may be a powerful analytical tool for investigating effects of ageing in a LIB.

4.2 Polymer electrolyte fuel cells

Paper 3 studies the operation of a PEFC which is assumed to be fed with reactants at such high stoichiometric rates that it can be described by a one-dimensional version of the presented physical model. Emphasis is put on how spatially resolved porous electrodes and nonequilibrium water transport across the interface between the gas phase and the ionic conductor affect the model results for the performance of the cell. Here, the performance of the cell is characterised by polarisation curves, that is plots of the cell potential, E_{cell}, against the cell current density, i_{cell}. The effect of the porous electrodes on the polarisation curve of the cell is investigated by changing their thicknesses ($h_{a/cpe}$) while keeping their total interfacial surface areas constant, see Fig. 4.5. Increasing their thicknesses increases the cell resistance, leading to an increase in the slope of the polarisation curve for intermediate current densities, and decreases the limiting current density. This result suggests that the porous electrodes cannot be approximated as planar electrodes. The effect of the nonequilibrium water transport is difficult to predict as it counteracts both water absorption and desorption and thus hinders both the hydration and the

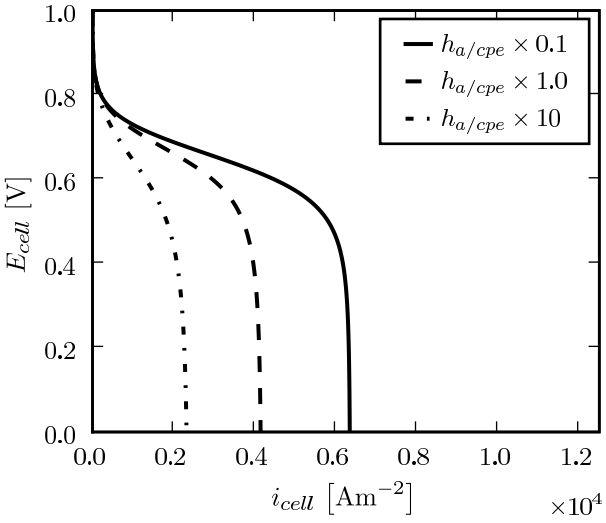

Figure 4.5: Influence of the anode and the cathode porous electrode thickness ($h_{a/cpe}$) on the polarisation curve of the cell; in changing $h_{a/cpe}$, the total interfacial surface areas of the porous electrodes are held constant.

dehydration of the ionic conductor. The impact of changing the mass transfer coefficients for absorption and desorption ($B_{ka/d}$) on the polarisation curve of the cell is shown in Fig. 4.6. Indeed, as the mass transfer coefficients increase, the performance of the cell first decreases and then increases again.

In order to understand the limiting behaviour of the current density, it is necessary to look at the profile of the content of water in the ionic conductor, λ. In Fig. 4.7, the water content is plotted against the dimensionless cell normal coordinate, $\bar{z}$, for different cell potentials. Here, the coordinate is made dimensionless in each domain using the corresponding domain thickness, its origin being placed in the centre of the membrane, such that $-1.5 < \bar{z} < -0.5$ represents the anode porous electrode, $-0.5 < \bar{z} < 0.5$ the membrane and $0.5 < \bar{z} < 1.5$ the cathode porous electrode. The water drag effect and the production of water on the cathode side create a gradient in the water content from the anode to the cathode as the cell potential decreases and thus the cell current density increases. At the lowest cell potential shown, the cell current density has almost reached its limiting value and it can be seen that the water content in the anode porous electrode is only slightly larger than the conduction threshold of the ionic conductor, that is $\lambda \approx 0.625$. This result shows that the limiting behaviour of the current density is due to the dehydration of the anode.

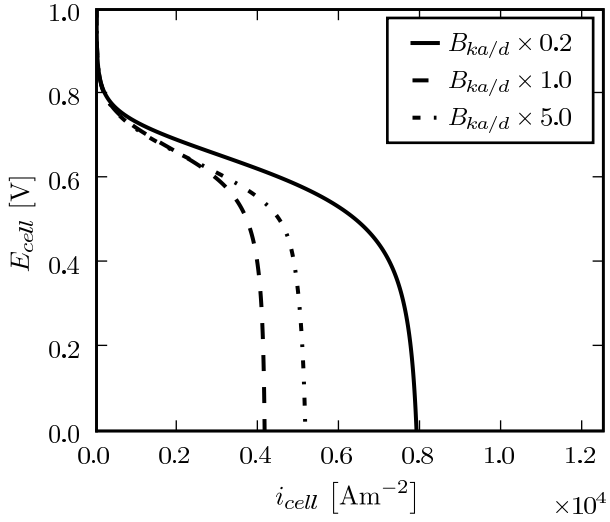

Figure 4.6: Influence of the mass transfer coefficient for absorption and desorption of water of the interface between the gas phase and the ionic conductor ($B_{ka/d}$) on the polarisation curve of the cell.

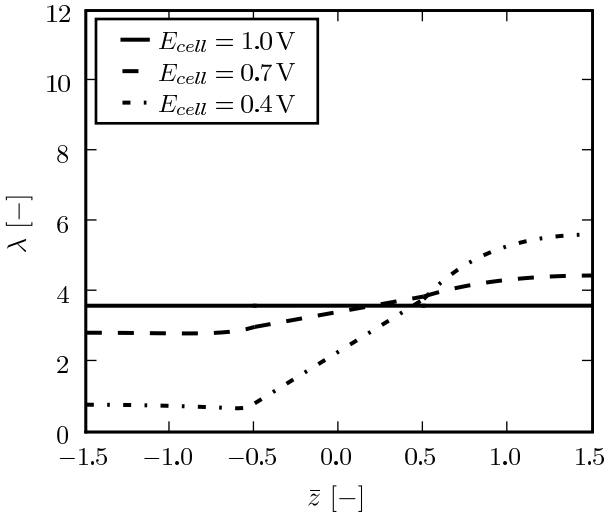

Figure 4.7: Profile of the content of water in the ionic conductor for different cell potentials.

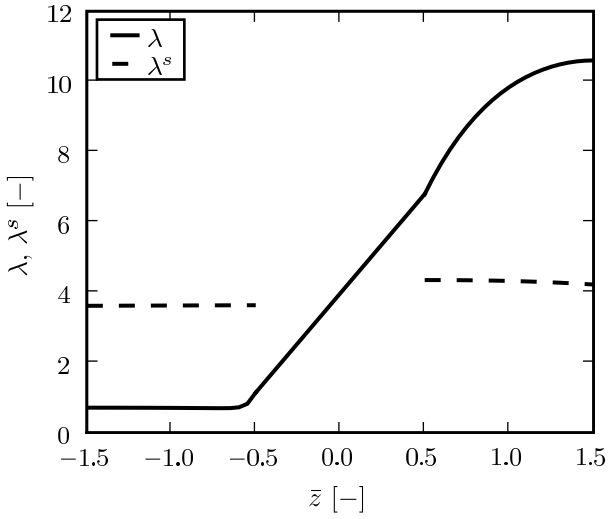

Figure 4.8: Profile of the content and the saturated content of water in the ionic conductor for $E_{cell} = 0.4\,\mathrm{V}$ and $B_{ka/d} \times 0.2$.

The minimal performance encountered in Fig. 4.6 can be explained by studying the profiles of the content and the saturated content, denoted by a superscript s, of water in the ionic conductor for a cell potential at which the limiting current density behaviour sets in and the cases investigated in Fig. 4.6, see Figs. 4.8-4.10. As the mass transfer coefficient increases, the water content profile approaches that of the saturated water content on both the anode and the cathode side. However, the main decrease in water content on the cathode side precedes the main increase in water content on the anode side, leading to the minimal performance behaviour observed. It is worth noting that the saturated water content is quite uniform throughout the porous electrodes and that it does not deviate far from its value at very low cell current densities. Since the saturated water content essentially corresponds to the mole fraction of water in the gas phase, it can be concluded that the mass transport in the gas phase is rapid in comparison with the mass transport in the ionic conductor and the interfacial mass transport between the phases.

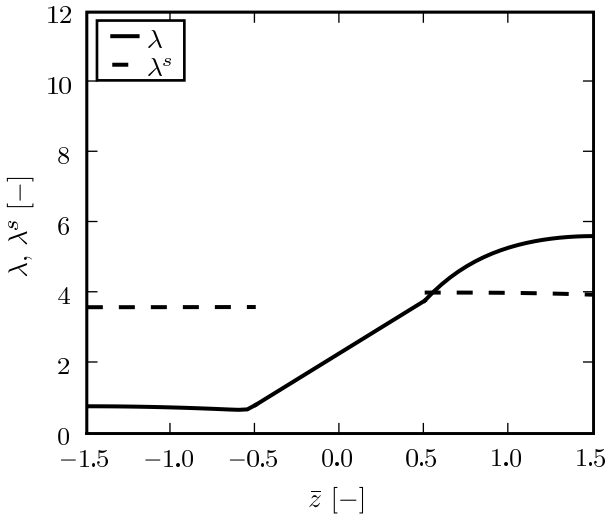

Figure 4.9: Profile of the content and the saturated content of water in the ionic conductor for $E_{cell} = 0.4\,\mathrm{V}$ and $B_{ka/d} \times 1.0$.

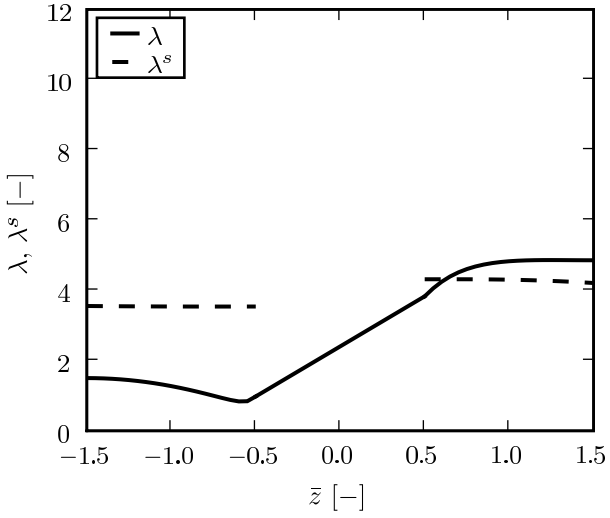

Figure 4.10: Profile of the content and the saturated content of water in the ionic conductor for $E_{cell} = 0.4\,\mathrm{V}$ and $B_{ka/d} \times 5.0$.

CHAPTER 5

Conclusions

Validated modelling proved to be a valuable tool in studying the effects of ageing in a LIB. The model formulation and the investigated ageing scenarios were based on electrochemical and material characterisation studies and experimental observations. Using a hybrid genetic optimisation technique to fit the model to the experimental data resulted in a good agreement between the fitted and the experimental impedance spectra and parameter values which both agree well with literature values and support the suggested ageing scenario. The results cannot rule out other ageing scenarios but the combination of a physically based model, significant experimental data and a reliable optimisation strategy provided a tool which can be used to test an ageing hypothesis for its admissibility.

A steady state PEFC model that resolves the porous electrodes and accounts for nonequilibrium water transport was formulated and investigated in a one-dimensional configuration. The results suggest that the porous electrodes cannot be approximated as planar electrodes. Furthermore, the transport of water in the cell is further complicated by dropping the assumption of equilibrium of water between the gas phase and the ionic conductor. The mass transfer resistance for the transport of water across the interface between the gas phase and the ionic conductor impedes both the hydration and the dehydration of the ionic conductor and can thus both increase and decrease the cell performance. This was demonstrated by gradually decreasing the resistance which first decreased and then increased the limiting current density of the cell.

CHAPTER 6

Future Work

The PEFC model presented in Paper 3 has been studied in a one-dimensional configuration for a range of parameter values. However, the model still contains a number of parameters which affect the water transport and other aspects of the cell operation and the effects of which have not been investigated. In addition, considering the model in higher dimensions is expected to add further phenomena which need to be analysed. Regarding the use of the model in higher dimensions, it would be of interest to theoretically establish the meshing requirements in the cell normal direction in the porous electrodes at their boundaries in order to deal with the singular behaviour of their source terms observed in Paper 3. Thus there are many aspects of the presented model formulation which require further theoretical work.

As noted in Paper 3, some of the parameter values of the model probably need to be adjusted. Furthermore, so far no steps have been undertaken to validate the model against experimental data. It would be desirable to design a suitable series of experiments and adjust the parameter values of the model by fitting it to the resulting experimental data. In addition, a comparison with experimental data would hopefully allow at least a partial validation of the model. Prior to any parameter fitting or model validation, however, it would be beneficial to subject the model formulation to a rigorous nondimensional analysis in order to both mathematically reduce it and determine the combinations of parameters having the strongest impact on the modelling results.

Acknowledgements

I would like to express my gratitude to my supervisors, Docent Michael Vynnycky and Docent Anders Dahlkild. In particular, I would like to thank Docent Michael Vynnycky for support, encouragement and patience.

Financial support from the Swedish Foundation for Strategic Environmental Research (MISTRA) is gratefully acknowledged. Furthermore, part of this work was done during a visit at the Japan Aerospace Exploration Agency (JAXA) which was funded by a scholarship from the Sweden-Japan Foundation (SJF) and JAXA. I would like to thank SJF and JAXA for the financial support and the members of the Sone and the Tajima Laboratory at JAXA for hospitality.

I feel indebted to Dr. Shelley Brown for an inspiring, productive and enjoyable collaboration. I would also like to thank Dr. Carl-Ola Danielsson and Dr. Shelley Brown for many valuable discussions about electrochemistry and related subjects.

Trying to mention all friends and colleagues at KTH and JAXA who have supported me in one way or another and who have displayed great tolerance and generously offered kindness in difficult times seems like a formidable task. I hope that you know who you are and that you accept my thanks. A few people cannot, however, remain unmentioned. Thank you, Linus Marstorp, Bengt Fallenius, Shelley Brown, Edmond So and Andreas Vallgren.

Finally, I would like to thank my family, Ingrid, Anders, Fredrik and Marta, for all their support and patience.

References

1. R. Taylor and R. Krishna, *Multicomponent Mass Transfer*, John Wiley & Sons, 1st ed. (1993).

2. J. Newman and K. E. Thomas-Alyea, *Electrochemical Systems*, John Wiley & Sons, 3rd ed. (2004).

3. R. Jackson, *Transport in porous catalysts*, Elsevier, 1st ed. (1977).

4. T. E. Springer, T. A. Zawodzinski, and S. Gottesfeld, *J. Electrochem. Soc.*, **138**, 2334 (1991).

5. P. Futerko and I.-M. Hsing, *J. Electrochem. Soc.*, **146**, 2049 (1999).

6. S. Ge, X. Li, B. Yi, and I.-M. Hsing, *J. Electrochem. Soc.*, **152**, A1149 (2005).

7. S. Whitaker, *The Method of Volume Averaging*, Kluwer Academic Publishers, 1st ed. (1998).

8. D. A. G. Bruggeman, *Ann. Phys.*, **416**, 636 (1935).

9. R. E. De La Rue and C. W. Tobias, *J. Electrochem. Soc.*, **106**, 827 (1959).

10. E. Barsoukov and J. R. Macdonald, editors, *Impedance Spectroscopy: Theory, Experiment, and Applications*, John Wiley & Sons, 2nd ed. (2005).

11. J. C. Spall, *Introduction to Stochastic Search and Optimization: Estimation, Simulation, and Control*, John Wiley & Sons, 1st ed. (2003).

12. W. H. Press, S. A. Teukolsky, W. T. Vetterling, and B. P. Flannery, *Numerical Recipes in C: The Art of Scientific Computing*, Cambridge University Press, 2nd ed. (1992).

Part II

Papers